

LEVELS OF  $^{230}\text{Th}$  AND  $^{230}\text{U}$  FED IN THE DECAY OF  $^{230}\text{Pa}$ 

BY W. KURCEWICZ, K. STRYCNIEWICZ, J. ŻYLICZ

Institute of Nuclear Research, Department of Physics, Świerk near Warsaw\*\*

S. CHOJNACKI\*, T. MOREK\* AND I. YUTLANDOV

Joint Institute of Nuclear Research, Dubna, USSR

(Received December 8, 1970)

The  $^{230}\text{Pa}$  decay to levels of  $^{230}\text{Th}$  and  $^{230}\text{U}$  is investigated using Si(Li) and Ge(Li) spectrometers for singles-spectra measurements, and a Ge(Li) spectrometer combined with a six-gap  $\beta$  spectrometer or with a NaI(Tl) detector for coincidence measurements. The decay scheme is proposed which accounts for all but one of the 50 transitions observed in the present investigation. The following bands of the  $^{230}\text{Th}$  excited states are established or proposed (in parentheses: level energies in keV, spin values and parities of the levels): the ground-state band (53.19,  $2^+$  and 174.12,  $4^+$ ), the quadrupole bands ( $\beta$ : 634.7,  $0^+$  and 677.8,  $2^+$ ;  $\gamma$ : 781.4,  $2^+$  and 825.4,  $3^+$ ;  $\beta + \gamma$  (?): 1009.61,  $2^+$  and 1052.6,  $3^+$ ) and the octupole bands ( $K^\pi = 0^-$ : 508.20,  $1^-$  and 571.71,  $3^-$ ;  $K^\pi = 1^-$ : 951.91,  $1^-$ ; 971.70,  $2^-$  and 1012.2,  $3^-$ ;  $K^\pi = 2^-$ : 1079.20,  $2^-$  and 1127.85,  $3^-$ ). The  $^{230}\text{Pa} \rightarrow ^{230}\text{Th}$  decay energy,  $Q$ , is deduced from the measured relative probabilities of the  $K$  capture transitions to several excited states in  $^{230}\text{Th}$ :  $Q = 1315^{+15}_{-10}$  keV. For  $^{230}\text{U}$ , the first excited  $2^+$  state is observed at 51.72 keV and the bandhead state of the  $K^\pi = 0^-$  octupole band is proposed at 366.5 keV. The experimental data are discussed in terms of nuclear models, with emphasis on the band-mixing effects.

## 1. Introduction

Earlier investigations on the  $^{230}\text{Pa}$  decay have been surveyed by Hyde *et al.* [1]; the main results can also be found in Ref. [2]. The 17.7 d  $^{230}\text{Pa}$  nuclide decays in about 90% to  $^{230}\text{Th}$  *via* electron capture and in about 10% to  $^{230}\text{U}$  by  $\beta$  transition. A low-intensity  $\alpha$  branch is also known. The data on the scheme of  $^{230}\text{Th}$  levels fed in the EC decay of  $^{230}\text{Pa}$  are mainly due to Nielsen *et al.* [3], who carried out a study by the scintillation technique and a six-gap  $\beta$  spectrometer, including  $e\text{-}\gamma$  coincidence measurements. For  $^{230}\text{U}$ , only one excited state has been reported [2] to be fed in the  $\beta$ -decay of  $^{230}\text{Pa}$ .

\* Permanent address: Warsaw University, Warsaw, Poland.

\*\* Address: Instytut Badań Jądrowych, Zakład IA, Świerk k/Otwocka, Poland.

In the present work, investigations of the  $^{230}\text{Pa}$  decay were undertaken with the hope that, by the extensive use of semiconductor spectrometers in singles and coincidence measurements, it would be possible to reach further, more complete, knowledge of the properties of the  $^{230}\text{Th}$  and  $^{230}\text{U}$  levels. Some preliminary results of this study were already presented in Ref. [4]. In the construction of the decay scheme some  $\gamma$ -ray data obtained with Ge(Li) spectrometers by Briand *et al.* [5] were also taken into account. The results are discussed in terms of current models for collective nuclear excitations.

## 2. Source preparation

About 1 g of thorium foil was bombarded for 3 to 6 hours with 100 MeV protons in the JINR synchrocyclotron at Dubna. To enable studies of the  $^{228}\text{Pa}$  decay [6], the protactinium fraction was separated from the target directly after irradiation by the method described by Hill [7]. A few weeks later, in addition to the  $^{230}\text{Pa}$  activity to be studied, the sample of protactinium contained  $^{233}\text{Pa}$  and some decay products, mainly  $^{228}\text{Th}$  and descendants. The protactinium activity was purified by means of an anion exchange column. The sources were prepared by the microcolumn technique [8].

## 3. Gamma-ray spectrum

Preliminary measurements of the  $\gamma$ -ray spectrum included several runs performed during the period of three months after source production in order to identify lines belonging to  $^{230}\text{Pa}$  and to determine their energies and intensities. These measurements were carried out at Dubna, mainly with the use of a 5 cm<sup>3</sup> Ge(Li) detector and a 4096 channel analyser. The source used then (and only this one) was not chemically purified and lines of the  $^{228}\text{Th}$  radioactive chain appearing in the spectra were used as internal standards for energy calibration. A source of  $^{226}\text{Ra}$  was used to determine the efficiency curve. In the "old" source spectra some lines of the  $^{230}\text{U}$  decay chain were observed.

In the measurements performed at Świerk, a 5.6 cm<sup>3</sup> Ge(Li) detector placed in a low-background lead shielding and a 512-channel analyser with a biased amplifier were used. These measurements were made in order to find low-intensity lines belonging to the  $^{230}\text{Pa}$  activity. The spectra are shown in Fig. 1.

The low-energy part of the  $\gamma$ -ray spectrum was precisely studied using the facilities at the University of Aarhus: a high-resolution X-ray Ge(Li) spectrometer and a 4096 channel analyser. The energies of X-rays and of the  $^{233}\text{Pa}$   $\gamma$  lines were used as calibration standards. The efficiency curve used was determined by the Aarhus group. A section of the spectrum is shown in Fig. 2 (see also insert (b) to Fig. 1). Also, some measurements of the high-energy part of the  $\gamma$ -ray spectrum were carried out in Aarhus with a 20 cm<sup>3</sup> Ge(Li) detector. Emphasis was put on the precision determination of the  $\gamma$ -ray energies from the measurement with a  $^{230}\text{Pa} + ^{110\text{m}}\text{Ag}$  source (see insert (c) to Fig. 1). The energy and intensity data for  $\gamma$ -rays of  $^{110\text{m}}\text{Ag}$  were taken from Ref. [9].

The results of the  $\gamma$ -ray spectra measurements are listed in Table I. The energies of  $\gamma$  transitions determined in the present work are in a very good agreement with those of Briand

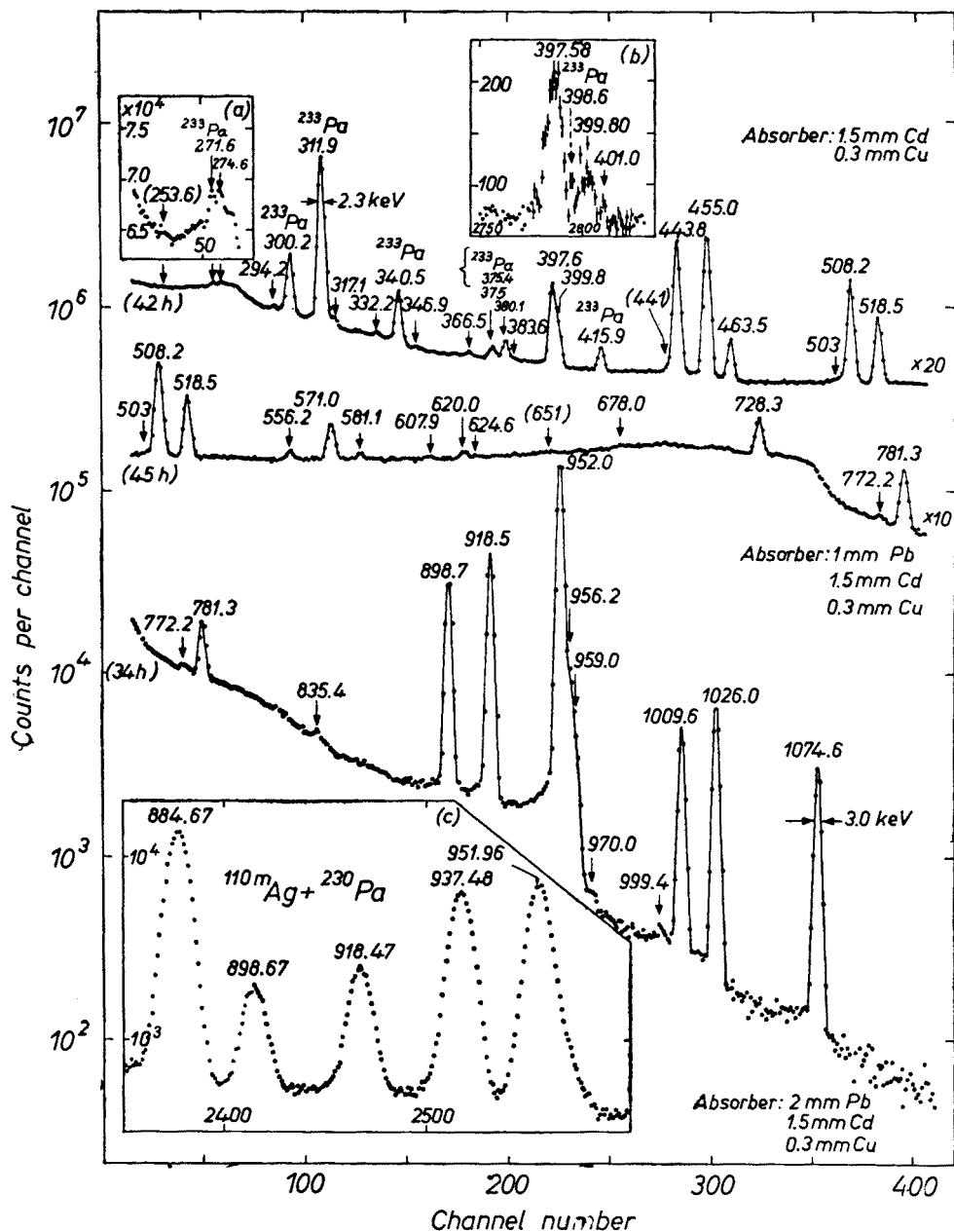


Fig. 1. Gamma-ray spectrum in the range above 250 keV measured with a 5.6 cm<sup>3</sup> Ge(Li) detector. Inserts: (a) section of spectrum plotted linearly; (b) composite peak at  $\approx 400$  keV, resolved with the use of a X-ray detector; (c) high-energy part of the  $^{110\text{m}}\text{Ag} + ^{230}\text{Pa}$   $\gamma$  spectrum measured with a  $\approx 20$  cm<sup>3</sup> Ge(Li) detector

TABLE I

Energies and relative intensities of  $\gamma$ -rays

$E_{\gamma}^a$		$I_{\gamma}^{a, b}$	
Ref. [5]	this work	Ref. [5]	this work
	<i>KX-rays</i> Th		11500 (800)
	51.72 (4)		4.1 (12)
53.15	53.19 (2)	16.7	49 (4)
120.82	120.93 (2)	41.7	78 (6)
	228.8 (6)		$\leq 4$
253.30	253.6 (9)	3.9	$\sim 3.5$
274.25	274.6 (9)	15.0	20 (5) <sup>c</sup>
	294.2 (9)		16 (5) <sup>c</sup>
297.8		16.7	
302.2		2.2	
314.8		16.7	
316.9	317.1 (3)	30.6	28 (6)
331.9	332.2 (4)	8.3	15 (3)
	(346.9)		$\leq 5$
366.55	366.5 (6)	12.8	16 (5)
374.7	375 (1) <sup>c</sup>	11.1	5.5 (14) <sup>c</sup>
	375 (1) <sup>c</sup>		$\sim 2^c$
380.15	380.13 (20)	63.9	50 (10)
397.71	397.58 (20)	328	370 (30)
399.95	399.8 (6)	117	117 (23)
	401.0 (8)		5.5 (16) <sup>c</sup>
440.8	441 (1) <sup>c</sup>	13.9	26 (9) <sup>c</sup>
443.77	443.80 (10)	1000	1000
	450 (1) <sup>c</sup>		$\sim 2^c$
454.90	455.02 (8)	1150	1110 (60)
463.57	463.54 (10)	144	159 (10)
	503.0 (10)		12 (4)
508.17	508.20 (8)	683	653 (78) <sup>c</sup>
	508 (1) <sup>c</sup>		42 (12) <sup>c</sup>
518.50	518.48 (8)	305	368 (25)
555.8	556.18 (10)	38.9	38 (4)
571.26	571.03 (10)	194	204 (10)
581.45	581.1 (4)	22.2	21 (5)
	607.9 (9)		13 (3)
619.69	620.0 (4)	52.8	37 (5)
	624.6 (4)		8.3 (16)
	635.0		$\leq 2$
	(651)		$\leq 4$
	678.0 (10)		$\approx 5$
728.17	728.29 (12)	344	315 (16)
772.20	772.2 (7)	26.1	14 (3)
781.38	781.32 (12)	267	255 (15)
	835.4 (7)		12 (2)

Table I (continued)

$E_\gamma^a$		$I_\gamma^{a,b}$	
Ref. [5]	this work	Ref. [5]	this work
898.53	898.67 (6)	1106	1010 (50)
918.43	918.47 (6)	1617	1450 (70)
951.90	951.96 (6)	5560	5230 (250)
	954 (1) <sup>c</sup>		30 (7) <sup>c</sup>
956.34	956.2 (5)	356	310 (78) <sup>d</sup>
959.50	959.0 (8)	94	130 (40) <sup>d</sup>
	970 (1)		2.5 (8)
	999.4 (10)		2.2 (7)
1009.44	1009.61 (20)	211	192 (10)
1026.06	1025.99 (20)	278	254 (13)
1074.75	1074.64 (20)	139	127 (6)

<sup>a</sup> The figures in parentheses correspond to the uncertainty in the last digits of the main number.  
<sup>b</sup> Data from Ref. [5] renormalized by the present authors.  
<sup>c</sup> Data from the  $e\text{-}\gamma$  coincidence measurements.  
<sup>d</sup> Joint intensity of these two lines obtained in the  $e\text{-}\gamma$  coincidence measurement is equal to 526 (80).

*et al.* [5]. The agreement between the intensity data from these two studies is rather good, except for the low-energy lines. The relative intensities of the 53.19 and 120.93 keV lines determined in the present study are about twice those obtained by Briand *et al.*

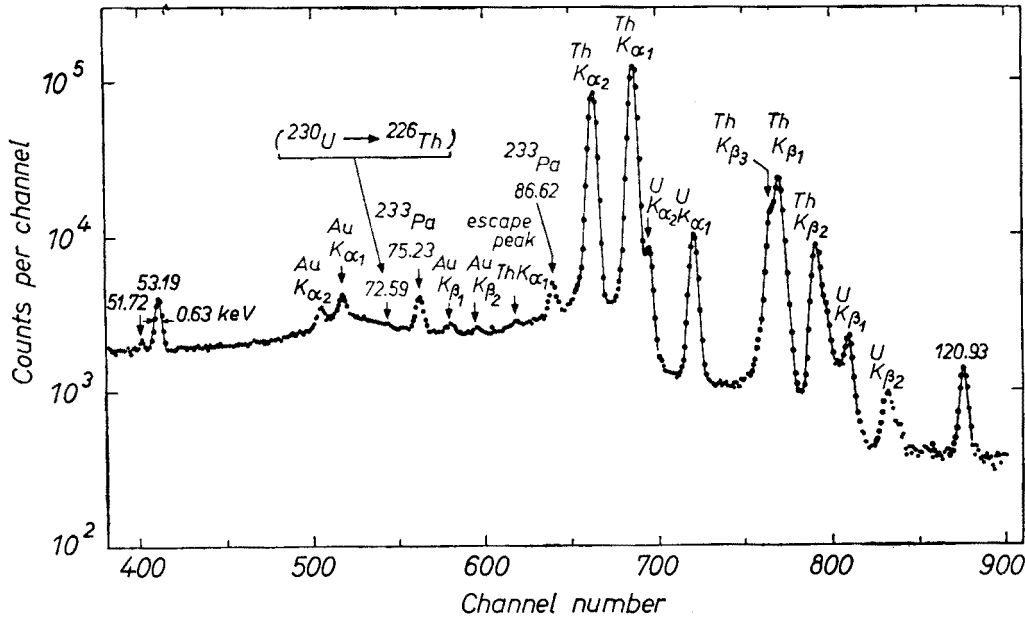


Fig. 2. Part of the X-ray and low-energy  $\gamma$ -ray spectrum measured with a high-resolution X-ray Ge(Li) detector

#### 4. Spectrum of conversion electrons and multipolarity assignments

The spectrum of internal conversion electrons was studied using a  $\beta$  spectrometer with a Si(Li) detector and a system of diaphragms placed in a homogeneous magnetic field. In this spectrometer electrons are focused on the surface of the detector with the zero dispersion. A 15 mm lead shielding between the source and detector provides a partial protection of the detector against  $\gamma$  radiation from the source. The system of diaphragms makes it possible to select a desired energy range of electrons for investigations. A detailed description of the spectrometer will be given in a separate publication [10].

The depth of the active volume of the Si(Li) detector used in the present work was 3 mm. The energy resolution of this detector was 3 keV for 624 keV electrons from a  $^{137}\text{Cs}$  source. The  $^{230}\text{Pa}$  measurements were performed for three partly overlapping electron-energy intervals, using a 512-channel analyser with a biased amplifier. The spectrum in the high-energy interval is shown in Fig. 3.

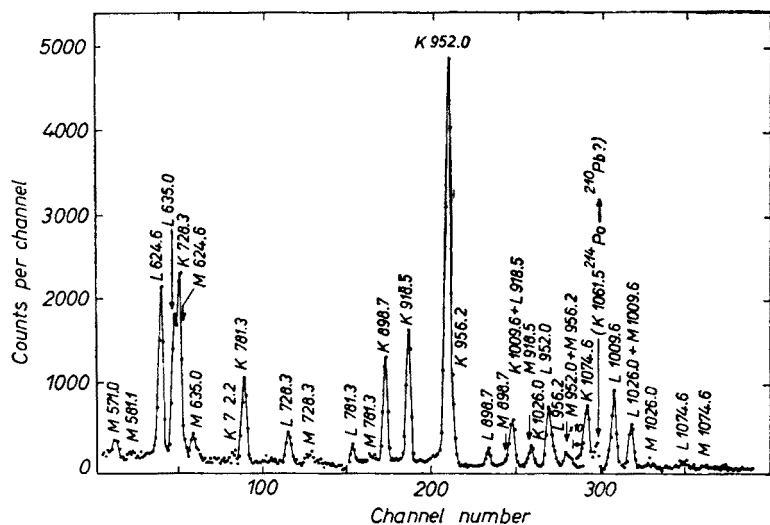


Fig. 3. High-energy part of the spectrum of internal-conversion electrons measured using the  $\beta$  spectrometer with a Si(Li) detector in a homogeneous magnetic field. The background due to  $\gamma$ -rays has been subtracted

The low-intensity  $K$ -conversion line of the 366.5 keV transition was found (Fig. 4) in a special measurement in which the intense electron lines were suppressed by the use of the spectrometer diaphragms. From the energy value determined for this line and from the electron binding energies in the  $K$  shell for U and Th it may be concluded that the 366.5 keV transition occurs in  $^{230}\text{U}$ .

The intensities of internal-conversion lines determined in the present work and those from Ref. [3] are listed in Table II. The errors quoted for the present-work data do not include uncertainty in the spectrometer-transmission curve. One has to consider, therefore, the possibility of additional systematic errors which for the low-energy lines may amount to 10–20%.

TABLE II

Internal-conversion data and multipolarity assignments

Transition energy (keV)		Relative intensity of conversion electrons <sup>a</sup>			Experimental ICC <sup>d</sup> this work		Multipolar-ity
		<i>K</i> lines		<i>L</i> lines			
Ref.[3]	this work	<sup>b</sup>	this work	this work	$\alpha_K$	$\alpha_L$	
53	53.2			108200 <sup>b</sup>		9.9(1) <sup>e</sup>	<i>E2</i> <sup>g</sup>
122	120.9			3530 <sup>b</sup>		1.9 (0) <sup>f</sup>	<i>E2</i> <sup>g</sup>
230	228.8	1150	1020 (82)	256 (23)	$\geq 13$ (0)	$\geq 2.9$ (0)	<i>E0</i>
	366.5		$\leq 9.8$		$\leq 2.74$ (-2)		( <i>E1</i> )
379	380.1	58.8	35.5 (116)		(3.2 $\pm$ 1.2 )(-2)		( <i>E2</i> )
398	397.6			} 148 (16)			
401	399.8	559				(4.7 $\pm$ 1.1)(-2)	<i>E2</i> + <i>M1</i>
	441		233 (70)		(4.0 $\pm$ 2.0)(-1)		<i>E2</i> + <i>M1</i>
444	443.8	3265	2910 (290)	700 (47)	(1.30 $\pm$ 0.17)(-1)	(3.1 $\pm$ 0.3)(-2)	<i>E2</i> + <i>M1</i>
456	455.0	244	198 (42)		(8.0 $\pm$ 2.4)(-3)		<i>E1</i>
464	463.5	559	488 (37)		(1.38 $\pm$ 0.19)(-1)		<i>E2</i> + <i>M1</i>
508	508.2	138	110 (29)		(7.0 $\pm$ 2.1)(-3)		<i>E1</i>
520	518.5	44	59 (9)		(7.3 $\pm$ 1.8)(-3)		<i>E1</i>
	556.2			15.3 (23)		(1.8 $\pm$ 0.3)(-2)	<i>E2</i> + <i>M1</i>
572	571.0	79	113 (10)	35.0 (35)	(2.49 $\pm$ 0.35)(-2)	(7.8 $\pm$ 0.9)(-3)	<i>E2</i>
	581.1		9.0 (23)		(1.92 $\pm$ 0.67)(-2)		<i>E2</i>
	620.0		16.6 (65)		(2.0 $\pm$ 1.0)(-2)		<i>E2</i>
624	624.6	483	498 (40)	116 (7)	(2.7 $\pm$ 0.6 )( 0)	(6.5 $\pm$ 0.4)(-3)	<i>E0</i> + <i>E2</i>
634	635.0	350	349 (31)		$\geq 7.8$ (0)		<i>E0</i>
730	728.3	82.3	98 (12)	25.8 (29)	(1.40 $\pm$ 0.27)(-2)	(3.7 $\pm$ 0.4)(-3)	<i>E2</i>
	772.2		6.9 (15)		(2.2 $\pm$ 0.8)(-2)		<i>E2</i>
783	781.3	61.7	66.3 (66)	16.6 (23)	(1.17 $\pm$ 0.21)(-2)	(2.9 $\pm$ 0.4)(-3)	<i>E2</i>
901	898.8	82.3	77.2 (62)	15.2 (15)	(3.43 $\pm$ 0.48)(-3)	(6.8 $\pm$ 0.8)(-4)	<i>E1</i>
920	918.5	100	100	18.1 (13)	3.10 (-3) <sup>e</sup>	(5.6 $\pm$ 0.5)(-4)	<i>E1</i>
954	952.0	346	360 (41)		(3.10 $\pm$ 0.53)(-3)		<i>E1</i>
	956.8		41 (11)		(5.2 $\pm$ 1.4)(-3)		( <i>E2</i> )
1012	1009.6	32.3	25.6 (48)	7.2 (7)	(6.0 $\pm$ 1.5)(-3)	(1.7 $\pm$ 0.2)(-3)	<i>E2</i>
1027	1026.0	14.6	14 (2)		(2.47 $\pm$ 0.60)(-3)		<i>E1</i>
	1074.6		5.6 (8)		(2.0 $\pm$ 0.4)(-3)		<i>E1</i>

<sup>a</sup> The figures in parentheses correspond to the uncertainty in the last digits of the main number.<sup>b</sup> Data from Ref. [3] renormalized by the present authors.<sup>c</sup> Based on assumption of *E1* multipolarity for the 918.5 keV transition.<sup>d</sup> The figures in parentheses correspond to the powers of ten.<sup>e</sup> Theoretical  $\alpha_L$  is equal to 174.<sup>f</sup> Theoretical  $\alpha_L$  is equal to 3.45.<sup>g</sup> See the text for discussion of this assignment.

Table II also contains the data on the conversion coefficients and multipolarity assignments. To calculate the conversion coefficients, the  $\gamma$ -ray and conversion-line intensities were normalized by assuming the theoretical [11] *E1* conversion coefficient ( $3.1 \times 10^{-3}$ ) for

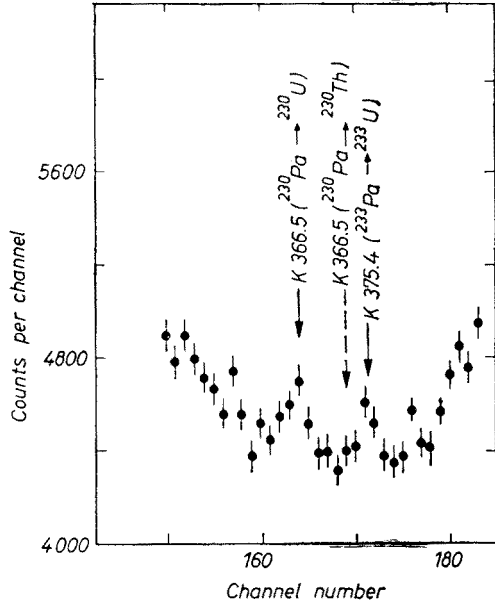


Fig. 4. The  $K$  366.5 line measured using the  $\beta$  spectrometer with a Si(Li) detector in a homogeneous magnetic field. It may be concluded that the 366.5 keV transition occurs in  $^{230}\text{U}$ , not in  $^{230}\text{Th}$

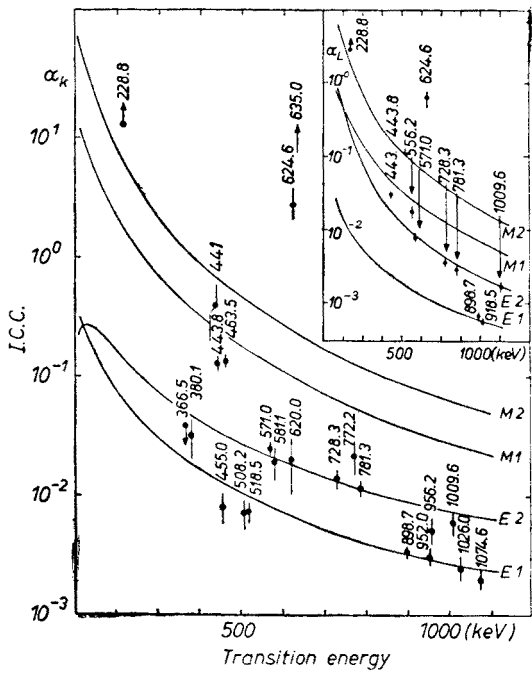


Fig. 5. Experimental and theoretical coefficients of internal conversion from  $K$  and  $L$  shells of  $\text{Th}$ . The  $\alpha_K$  value for the 366.5 keV transition is also given although this transition is assigned to  $^{230}\text{U}$  (see Fig. 4)



the 918.47 keV transition<sup>1</sup>. The coefficients obtained in this way are compared with the theoretical [11] predictions on Fig. 5. Multipolarity assignments are based in this comparison. The 51.72, 53.19 and 120.93 keV transitions should be *E2* if their placement in the decay scheme (*cf.* Fig. 12) is correct. This is supported by the *L*-subshell ratios measured using the six-gap spectrometer. If the  $\gamma$ -ray intensities as determined by Briand *et al.* [5] and the electron intensities from Ref. [3] are taken into account for the 53.19 and 120.93 keV transitions, a good agreement between the experimental and theoretical *E2* conversion coefficients is obtained. Contrary to this, the experimental conversion coefficients calculated for the transitions in question with the  $\gamma$ -ray intensities measured in the present work are almost two times lower than the theoretical values, Table II. The accuracy of the intensity data is discussed further in Section 7.1.

### 5. Electron-gamma coincidence studies

The measurements of  $\gamma$ -ray spectra in coincidence with conversion electrons were carried out with six-gap  $\beta$  spectrometer and a 5.6 cm<sup>3</sup> Ge(Li) detector placed at a distance of 1.5 cm from the source [12]. With three gaps employed, the  $\beta$  spectrometer was set at a resolution of  $\approx 1\%$  and a transmission of  $\approx 4\%$ . A fast-slow coincidence circuit with

TABLE III

Results of the *e*- $\gamma$  coincidence studies

Selected conversion line	Energies (keV) and intensities (in brackets) of coincident $\gamma$ lines
<i>M</i> 53.2	380(103 $\pm$ 40), 399(494 $\pm$ 75), 444(574 $\pm$ 80), 455(1340 $\pm$ 175), 463(243 $\pm$ 50), 508(125 $\pm$ 50), 518(390 $\pm$ 65), 556(84 $\pm$ 50), 571(147 $\pm$ 53), 728(275 $\pm$ 66), 899(876 $\pm$ 130), 918 (= 1450), 956(526 $\pm$ 80), 1026(191 $\pm$ 36), 1075(117 $\pm$ 25)
<i>L</i> 120.9	380(14.2 $\pm$ 3.7), 400(240 $\pm$ 48), 441(6.2 $\pm$ 2.1), 508(10.4 $\pm$ 3.0), 556(9.4 $\pm$ 2.6), 608(4.5 $\pm$ 2.0), 835(= 12), 954(29.5 $\pm$ 6.8)
<i>K</i> 228.8	608(<30), 728 (= 315), 781(205 $\pm$ 21)
<i>K</i> 397.6 + <i>K</i> 399.8	380(= 50), 398(248 $\pm$ 106), 441(27 $\pm$ 18), 455(57 $\pm$ 34), 508(70 $\pm$ 34), 518(294 $\pm$ 30)
<i>K</i> 443.8	455(= 1110), 508(653 $\pm$ 78)
<i>K</i> 624.6	275(24.7 $\pm$ 5.5), 294(20.3 $\pm$ 5.1), 317(6.7 $\pm$ 2.2), 332(= 15), 375(3.9 $\pm$ 1.2), 401(5.5 $\pm$ 1.6), 450( $\sim$ 2)
<i>K</i> 635.0	317(= 28), 375(5.5 $\pm$ 1.4)

<sup>1</sup> This was first proposed in Ref. [3].

a time-to-pulse height converter was used. Seven  $e\text{-}\gamma$  coincidence spectra were recorded for selected conversion lines. The results are presented in Figs 6-9 and Table III; they have been used to construct the decay scheme, Section 7.

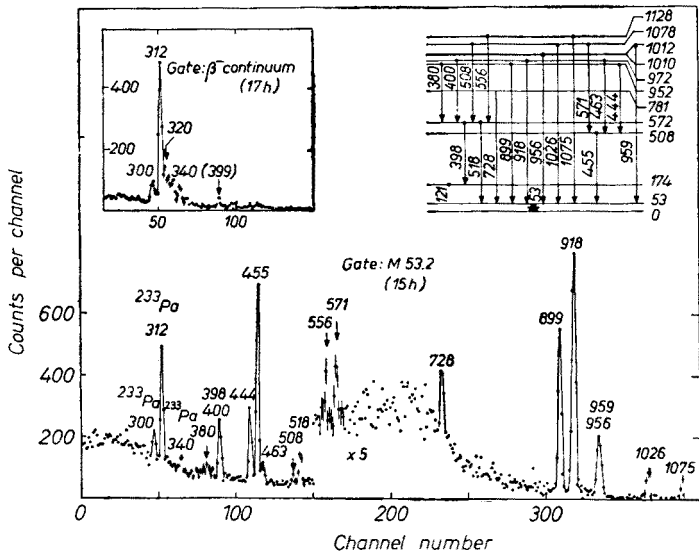


Fig. 6. Gamma-ray spectrum coincident with the  $M\ 53.2$  conversion electrons and its interpretation. Insert: the spectrum coincident with the  $^{233}\text{Pa}$   $\beta$  rays above the  $M\ 53.2$  line

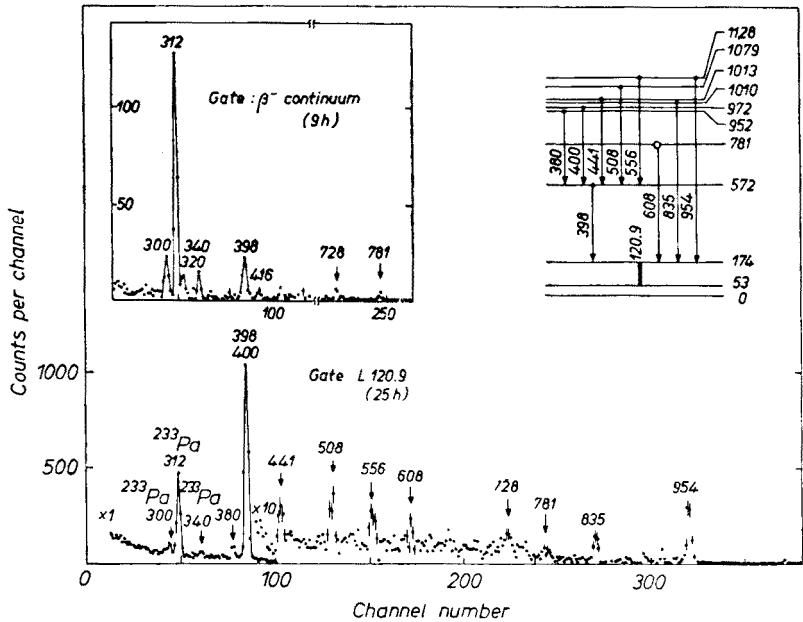


Fig. 7. Gamma-ray spectrum coincident with the  $L\ 120.9$  conversion electrons and its interpretation. Insert: the spectrum coincident with the  $^{233}\text{Pa}$   $\beta$  rays and with a tail of the  $K\ 228.8$  line (the origin of the  $\approx 320$  keV line in this spectrum is unknown)

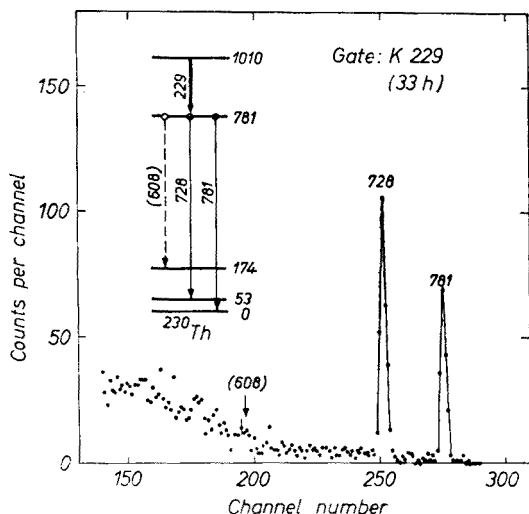


Fig. 8. Spectrum of  $\gamma$ -rays de-exciting the  $\gamma$  vibrational state, measured in coincidence with the  $K$  228.8 conversion line

#### 6. Determination of the electron-capture decay energy

The  $^{230}\text{Pa}$  decay energy  $Q_{\text{EC}}$  has been deduced from the analysis of the relative probability  $P_K$ , defined as the  $K/\text{total}$  capture ratio, for the electron-capture transitions to several excited states of  $^{230}\text{Th}$ .

To illustrate the procedure, consider two  $^{230}\text{Th}$  levels at the energy  $E_1$  and  $E_2$  fed directly by electron-capture transitions with the energy  $Q_{\text{EC}} - E_1$  and  $Q_{\text{EC}} - E_2$ . Let both levels be de-excited, at least in part, by  $\gamma$  transitions to the ground state or to the first-excited state. Such transitions may be in coincidence only with those  $KX$ -rays which are due to the  $K$ -capture process. If, for the transitions in question, the number of counts in the full-energy peaks are determined from the singles  $\gamma$ -ray spectrum ( $N_{\gamma_1}, N_{\gamma_2}$ ) and from the spectrum coincident with the  $KX$ -rays ( $N_{KX-\gamma_1}, N_{KX-\gamma_2}$ ), the ratio of the  $P_K$  values can be found using the relation:

$$\frac{P_K(Q_{\text{EC}} - E_1)}{P_K(Q_{\text{EC}} - E_2)} = \frac{N_{KX-\gamma_1}}{N_{KX-\gamma_2}} \frac{N_{\gamma_2}}{N_{\gamma_1}}$$

Then, to determine the  $Q_{\text{EC}}$  value, the theoretical [13], [14] dependence of  $P_K$  upon the transition energy  $Q_{\text{EC}} - E$  is used.

In this case,  $\gamma$ -rays of the energy 899, 918, 1010, 1026 and 1075 keV, de-exciting the levels at 952, 972, 1010, 1079 and 1128 keV, respectively (see Figs 10 and 12), were taken into account. The  $\gamma$ -ray spectrum was measured with a  $5.6 \text{ cm}^3$  Ge(Li) detector, while the  $KX$ -radiation was recorded in a  $3.8 \text{ cm diam.} \times 1.27 \text{ cm}$  NaI(Tl) counter. A fast-slow coincidence circuit with a time-to-pulse height converter was used. The analysis of the experimental data is shown in Fig. 11. It indicates that the decay energy  $Q_{\text{EC}}$  is  $1315^{+15}_{-10}$  keV.

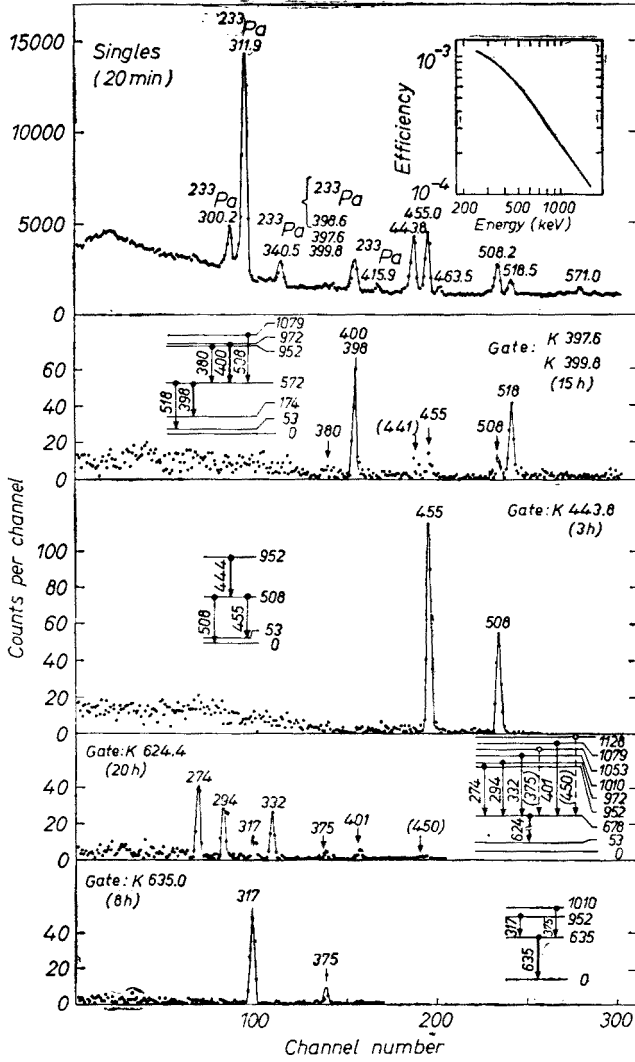


Fig. 9. Singles  $\gamma$ -ray spectrum and spectra measured in coincidence with the conversion lines, as indicated. Insert: the full-energy-peak efficiency curve for the Ge(Li) detector (with a 1 mm thick lead absorber)

7. The decay scheme

7.1. The  $^{230}\text{Pa} \rightarrow ^{230}\text{Th}$  decay

The electron-capture part of the  $^{230}\text{Pa}$  decay scheme proposed by Nielsen *et al.* [3] is fully confirmed. In addition, more than ten new low-intensity transitions have been placed between the  $^{230}\text{Th}$  levels introduced by those authors. Thirteen new transitions are believed to de-excite four levels at 1127.85, 1052.6, 1012.2 and 825.4 keV, introduced in the present work, as shown in Fig. 12.

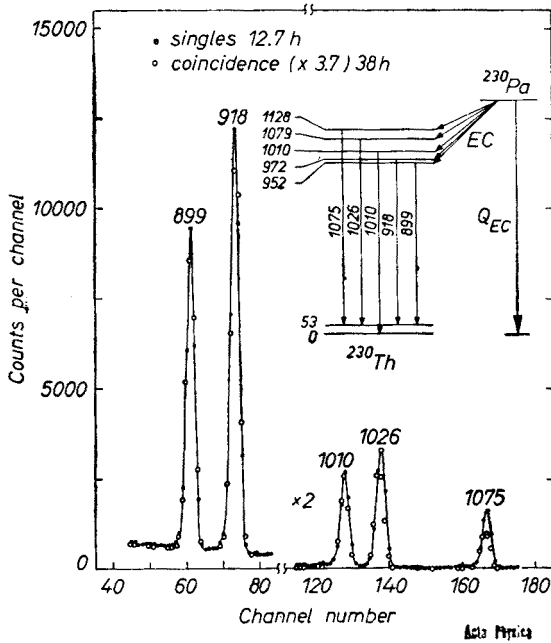


Fig. 10. Section of the singles  $\gamma$ -ray spectrum and the spectrum coincident with  $KX$ -rays (normalized to the intensity of the 899 keV line) and a fragment of the decay scheme

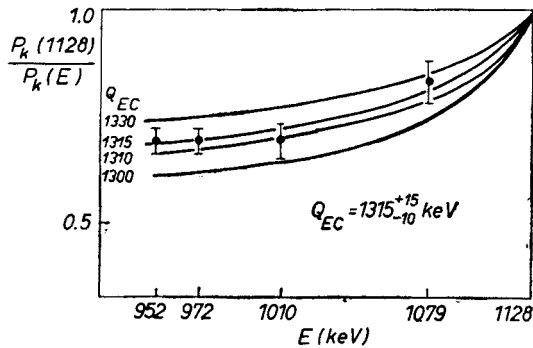


Fig. 11. Dependence of the  $P_K(1128)/P_K(E)$  ratio on the level energy  $E$  for various values of transition energy  $Q_{EC}$ . The experimental values of this ratio, obtained in coincidence measurements (see Fig. 10) are also presented

The 1127.85 keV level results unambiguously from the  $e\text{-}\gamma$  coincidence experiments and consideration of transition energy fits. The de-excitation pattern and, in particular, the multipolarity assignments to the 1074.64, 620.0 and 556.18 keV transitions establish the spin and parity for this level as  $3^-$ .

The 1052.6 keV level is suggested by a possible 375 keV transition in coincidence with the  $K$  624.6 electrons and the 999.4 keV transition that may connect this level with the first rotational state.

The 956.2 keV line, observed in the  $\gamma$ -ray spectrum coincident with the  $M$  53.2 transition, has an intensity higher than could be expected from the data on the singles  $\gamma$ -ray



spectrum. This intensity excess is assigned mainly to the 959.0 keV line. As the 959.0 keV line does not appear in the spectrum coincident with the  $L$  120.9 electrons, the existence of the 1012.2 keV level is implied. This level probably has negative parity, as it seems to decay by the 441 keV  $M1 + E2$  transition to the 571.71 keV  $3^-$  level.

The even parity level at 825.4 keV has been introduced on the basis of the energy fit of the 253.6, 302.2, 772.2  $E2$  and possible 651 keV transitions.

The assignment of spin 3 to the 1052.6, 1012.2 and 825.4 keV levels cannot be unambiguously deduced from the experiment. It is based on the interpretation of these levels as rotational states of the  $K^\pi = 2^+, 1^-$  and  $2^+$  bands, respectively (Section 8).

As the intensity of the  $\beta^-$  branch has been found to be  $8.4 \pm 1.3\%$  of  $^{230}\text{Pa}$  decays, the intensity of the EC decay is  $91.6 \mp 1.3\%$ . The latter intensity is shared between many individual EC transitions. The Th  $KX$ -ray intensity (Table I) has been taken into account when estimating the EC feeding of the  $^{230}\text{Th}$  ground state.

The intensities of the 53.19 and 120.93 keV transitions are mainly due to conversion electrons. If the intensities of the  $L$  53.2 and  $L$  120.9 lines reported in Ref. [3] (and corrected for the higher-shell conversion) are true, the 53.19 and 174.12 keV levels should be fed by internal and EC transitions with a surplus of 9 and 1%, respectively. It is concluded, therefore, that the  $L$  53.2 and  $L$  120.9 intensities from Ref. [3] (and also intensities of the corresponding  $\gamma$  lines from Ref. [5], see Section 3) are underrated. The intensities given in Fig. 12 for the 53.19 and 120.93 keV transitions have been calculated with the  $\gamma$ -ray data determined in the present work and theoretical  $E2$  conversion coefficients.

The EC branchings, the decay energy  $Q_{\text{EC}} = 1351^{+15}_{-10}$  keV and the theoretical EC data from Refs [13], [14] have been used to calculate  $\log ft$  values.

## 7.2. The $^{230}\text{Pa} \rightarrow ^{230}\text{U}$ decay

In the  $\beta^-$  decay of  $^{230}\text{Pa}$  at least two levels of  $^{230}\text{U}$  are fed: the already known [2] first rotational state at 51.72 keV and a new level proposed at 366.5 keV. The latter level has been introduced because the 366.5 keV transition has been assigned to  $^{230}\text{U}$  and in Ref. [5] a 314.8 keV transition is reported which may de-excite this level to the 51.72 keV state. As the 366.5 keV transition may be  $E1$ , the new level probably has spin 1 and odd parity.

The  $\beta^-$  branching of  $^{230}\text{Pa}$  has been determined by referring the intensity of the 324.6 keV transition of  $^{222}\text{Ra}$ , the decay product of the 20.8 d  $^{230}\text{U}$  activity, to the intensity of the 443.80 keV transition in  $^{230}\text{Th}$ . The 324.6 keV line was clearly visible in the  $\gamma$ -ray spectra measured with the "old" protactinium sources. Use was made of the known intensity of the 324.6 keV transition, which according to Peghaire [15] amounts to  $2.77 \pm 0.08\%$  of  $^{222}\text{Ra}$  decays. As a result, it was found that the  $\beta^-$  decay of  $^{230}\text{Pa}$  occurs at the rate of  $8.4 \pm 1.3\%$ . To calculate the  $\log ft$  values, the decay energy  $Q_{\beta^-}$  equal to 570 keV was assumed, in accordance with the result of the closed-energy-cycle analysis [2].

Fig. 12. The scheme of  $^{230}\text{Pa}$  decay to the levels of  $^{230}\text{Th}$  and  $^{230}\text{U}$ . The internal transitions established or suggested by coincidence measurements are marked with full and open circles, respectively. Crosses refer to the transitions placed on the basis of energy fits alone. The intensities (in parentheses) of the transitions are given in per cents of the total decays of  $^{230}\text{Pa}$ . The 297.8, 302.2 and 314.8 keV transitions have been observed by Briand *et al.* [5]. For further comments, see text and captions to Figs 13 and 14

8. Discussion

8.1. Even-parity states

The interpretation proposed for the even-parity states of  $^{230}\text{Th}$  is presented in Fig. 13. Apart from the ground-state band, the levels with excitation energy below 1 MeV shown in this figure are associated with  $\beta$  and  $\gamma$  vibrations. The 1009.61 keV level reveals some properties expected for the two-phonon  $\beta+\gamma$  vibrational state.

$A(\text{keV})$	$I^\pi$	$E(\text{keV})$	$K$	$n_\beta$	$n_\gamma$
$7.17 \pm 0.23$	$3^+$	$\frac{1052.6}{1009.61}$	2	(1)	(1)
	$2^+$				
$7.33 \pm 0.12$	$3^+$	$\frac{825.4}{781.4}$	2	0	1
	$2^+$				
$7.18 \pm 0.10$	$2^+$	$\frac{677.8}{634.7}$	0	1	0
	$0^+$				
	$4^+$	$\frac{174.12}{53.19}$	0	0	0
$8.65 \pm 0.003$	$2^+$				
	$0^+$				

Fig. 13. Interpretation of the  $^{230}\text{Th}$  even-parity states. Notation:  $A$  — inertial parameter,  $I^\pi$  — spin and parity,  $E$  — level energy,  $K$  — projection of spin on symmetry axis,  $n_\beta$  and  $n_\gamma$  — quantum numbers of  $\beta$  and  $\gamma$  oscillations

The  $K = 0$  assignment to the 634.7 keV  $0^+$  and 677.8 keV  $2^+$  levels is clearly established by their EO decays to the  $0^+$  and  $2^+$  levels of the ground-state band. For the analysis of EO transitions Rasmussen introduced the dimensionless parameter  $X$  (for definition and formulas, see Refs [16], [17]) which, in the case of  $\beta$  vibrations, is given by the expression  $X_\beta = 4\beta^2$ , while for transitions related to other possible  $0^+$  excitation modes is expected to have essentially different values. The quadrupole-deformation parameter  $\beta$  for  $^{230}\text{Th}$  is equal [18] to  $0.222 \pm 0.003$ , what yields  $X_\beta = 0.197 \pm 0.006$ . The values of  $X$  deduced from experiment for the 635.0 and 624.6 keV EO transitions are  $0.18 \pm 0.04$  and  $0.17 \pm 0.04$ , respectively. The agreement of  $X_\beta$  with the experimental results supports the interpretation of the 634.7 and 677.8 keV levels as members of the  $\beta$  band.

The calculations of the band-mixing parameter  $z_0$  for the  $\beta$  band have been performed with the assumption that the three  $\gamma$  transition de-exciting the 677.8 keV level are pure  $E2$ . The two  $z_0$  values deduced from the branching ratios, Table IV, are equal but have a large uncertainty. Hence, some  $M1$  admixture to the 624.6 keV  $E0 + E2$  transition cannot be excluded (see discussion in Ref. [19]). An upper limit of 26% is found for this admixture when the procedure proposed by Koksharova and Mihailov [20] is adopted. In this procedure, applied to the  $^{230}\text{Th}$  case, the value of the  $K$ -conversion coefficient for the 624.6 keV transi-



TABLE IV

Ratios of reduced probabilities of the  $E2$  transitions between even-parity states

Initial state		Final state		Transition energy (keV)	Reduced probabilities		Mixing parameter $z_{K_i}^a$
energy (keV)	$K_i I_i^{\pi_i}$	energy (keV)	$K_f I_f^{\pi_f}$		experiment this work	Alaga rule Ref. [24]	
678.8	0 2 <sup>+</sup>	0	0 0 <sup>+</sup>	678.0	$0.40 \pm 0.21$	0.70	$0.04 \pm 0.03$
		53.2	0 2 <sup>+</sup>	624.6	1	1	
		174.1	0 4 <sup>+</sup>	503	$4.3 \pm 1.7$	1.80	$0.04 \pm 0.02$
781.4	2 2 <sup>+</sup>	0	0 0 <sup>+</sup>	781.3	$0.57 \pm 0.05$	0.70	$0.036 \pm 0.015$
		53.2	0 2 <sup>+</sup>	728.3	1	1	
		174.1	0 4 <sup>+</sup>	607.9	$0.10 \pm 0.03$	0.05	$0.07 + 0.04$ $-0.03$
825.4	2 3 <sup>+</sup>	53.2	0 2 <sup>+</sup>	772.2	1	1	
		174.1	0 4 <sup>+</sup>	651	$\leq 0.56$	0.40	$\leq 0.03$
1009.6	2 2 <sup>+</sup>	0	0 0 <sup>+</sup>	1009.6	$0.47 \pm 0.12$	0.70	$0.068 \pm 0.040$
		53.2	0 2 <sup>+</sup>	956.2	1	1	
		174.1	0 4 <sup>+</sup>	835.4	$0.076 \pm 0.023$	0.05	$0.035 \pm 0.030$
1009.6	2 2 <sup>+</sup>	634.7	0 0 <sup>+</sup>	375	$0.20 \pm 0.06$	0.70	$0.23 \pm 0.06$
		677.8	0 2 <sup>+</sup>	332.2	1	1	

<sup>a</sup> See e.g. Ref. [25] for definitions and formulas; the  $z_2$  values for the transitions from the 1009.61 keV level are calculated in the same way as in the case of  $\gamma$  band.

tion is analysed, with the theoretical  $M1$  and  $E2$  conversion coefficients and experimental branching ratios for transitions de-exciting both members of the  $\beta$  band taken into account. The probabilities of the  $0^+ \rightarrow 0^+$  and  $2^+ \rightarrow 2^+$   $E0$  transitions are assumed to be equal.

The experimental values of the mixing parameter  $z_2$  obtained from the branching ratios of the transitions de-exciting the two levels of the  $\gamma$  band, Table IV, are close to those reported for the  $\gamma$  bands in the neighbouring nuclei  $^{228}\text{Th}$  (Ref. [21]),  $^{232}\text{U}$  (Ref. [22]) and  $^{234}\text{U}$  (Ref. [23]).

As could be expected for a two-phonon  $\beta + \gamma$  state, the 1009.61 keV level decays to the  $\gamma$ -vibrational level by an  $E0$  transition and to the levels of the  $\beta$  band by (presumably)  $E2$  transitions. However, contrary to the predictions for a pure two-phonon excitation, this level also decays by  $E2$  transitions to the ground-state band. The reduced probability of the 332.2 keV transition to the  $2^+$  level of the  $\beta$  band is only an order of magnitude larger than that for the 956.2 keV transition to the 53.19 keV  $2^+$  level. Moreover, in the simple model of harmonic nuclear vibrations the energy of a two-phonon  $\beta + \gamma$  state is equal to the sum of energies of the one-phonon  $\beta$  and  $\gamma$  excitations. The experimental value is much lower.

A  $2^+$  state revealing properties of the two-phonon  $\beta + \gamma$  vibration has also been observed [23] in  $^{234}\text{U}$ .

### 8.2. Odd-parity states

The odd-parity states of  $^{230}\text{Th}$  and  $^{230}\text{U}$  are interpreted as members of the octupole bands.

The  $^{230}\text{Th}$  states are assigned to the  $K^\pi = 0^-, 1^-$  and  $2^-$  bands as shown in Fig. 14. The inertial parameters  $A$  of these bands, calculated from the energies of two lowest levels for each band, are quite different. Also, the level interpreted as  $3^-$  in the  $K = 1$  band is much higher than expected from the  $E_{\text{rot}} = AI(I+1)$  formula. These anomalies are believed to result primarily from a strong Coriolis interaction of the bands. To reproduce approximately

$A$ (keV)	$E_{\text{exp}}$ (keV)	$E_{\text{calc.}}$ (keV)	$K$	$I^\pi$
$8.11 \pm 0.05$	1127.65	1113.31	2	$3^-$
	1079.20	1072.80	2	$2^-$
	1012.20	1018.61	1	$3^-$
	971.70	978.10	1	$2^-$
$4.95 \pm 0.03$	951.91	951.09	1	$1^-$
$6.35 \pm 0.01$	571.71	576.54	0	$3^-$
	508.20	509.02	0	$1^-$

Fig. 14. Negative-parity levels of  $^{230}\text{Th}$ . Notation:  $E_{\text{exp}}$  — experimental level energies,  $E_{\text{calc}}$  — unperturbed level energies deduced from the experimental ones through analysis of three-band Coriolis interaction (the perturbed energies calculated for the  $3^-$  states are: 571.65, 1008.2 and 1128.55 keV).  $A, K, I^\pi$  — see caption to Fig. 13

the experimental level energies, the general theory of the Coriolis effect has been applied to the case of three interacting bands and it has been assumed that the unperturbed  $A$  value is the same for all these bands. In addition to  $A$ , also the coupling matrix elements  $A_{01}$  and  $A_{12}$  (subscripts refer here to the  $K$  values) have to be considered as free parameters. However, for the sake of simplicity of the calculations, the experimental energies of the spin  $I = 1$  and  $I = 2$  levels have been used to find a relation between the parameter  $A_{01}$  and parameters  $A$  and  $A_{12}$  (very small experimental errors have been neglected). These latter parameters have been fixed by fitting the calculated energies of the spin  $I = 3$  levels to the experimental ones by use of the  $\chi^2$  function. This function reveals a deep minimum for the parameter values given in Table V, though the remaining differences between the calculated and experimental energies (see caption to Fig. 14) can hardly be explained by experimental uncertainties alone.

The experimental energies of the levels of the  $^{230}\text{Th}$  octupole bands are compared in Table VI with the theoretical results based on the microscopic theory [26–29]. For the band-head states the agreement between the experimental and calculated energies to within a few hundred keV or better is observed. Microscopic calculations accounting for the Coriolis interaction, performed by Neergård and Vogel [28], to some extent explain the properties

TABLE V

Matrix elements of the Coriolis interaction (in keV)

$A_{K, K+1}$	Experiment		Theory c
	a	b	
$A_{01}$	12.72	$20^{+5}_{-6}$	29.9
$A_{12}$	13.45	$16.1 \pm 1.3$	27.3

a From the analysis of the level-energy spacings. The inertial parameter  $A = 6.75$  keV.  
b From the analysis of the  $\log ft$  values.  
c The spherical-limit values calculated according to the formula given in Ref. [28].

TABLE VI

Energy levels of octupole bands in  $^{230}\text{Th}$

$K$	$I^\pi$	Energy (keV)				
		Experiment this work	Theory			
			Ref. [26]	Ref. [27]	a	Ref. [29]
0	1 <sup>-</sup>	508	510	760	370	510
	3 <sup>-</sup>	572			410	
1	1 <sup>-</sup>	952	1120	870	870	1000
	2 <sup>-</sup>	972			850	
	3 <sup>-</sup>	1012			920	
2	2 <sup>-</sup>	1079	1420	1160	980	1200
	3 <sup>-</sup>	1128			1080	
3	3 <sup>-</sup>			1580	1290	

a Approximate values read from Fig. 3 in Ref. [28].

of octupole bands. The strength of the interaction seems, however, to be somewhat overestimated by those authors, as indicated by the reversed order of the 1<sup>-</sup> and 2<sup>-</sup> states in the  $K = 1$  band (see also Table V).

An analysis of the EC and  $\beta^-$  branchings leads to the conclusion that the  $^{230}\text{Pa}$  ground state has spin  $I = 2$  and probably odd parity. As already pointed out in Ref. [1], this state may result from the coupling of the Nilsson orbitals: proton  $1/2^-(530)$  and neutron  $3/2^+(631)$ . If the initial state is assumed to be pure  $K = 2$ , one can obtain the values of the Coriolis coupling matrix elements from the  $\log ft$  data for EC transitions to the levels of octupole bands. The value of  $A_{01}$  has been deduced by comparing  $\log ft$  data for the EC transitions to the 951.91 and 508.20keV 1<sup>-</sup> states. It has been assumed that the  $K$ -forbiddenness of the transition to the second of these states is removed by an admixture of the first one.

TABLE VII

Selected  $\gamma$ -ray branching ratios for transitions de-exciting octupole bands

Initial state		Final state		Transition		Reduced branching ratios			Michailov parameter $\langle a \rangle$
energy (keV)	$K_i I_i^{\pi_i}$	energy (keV)	$K_f I_f^{\pi_f}$	energy (keV)	multipol.	experiment this work	Michailov formula <sup>a</sup> $a = 0_{av} \mid a = \langle a \rangle_{av}$		
508.2	0 1 <sup>-</sup>	53.2	0 2 <sup>+</sup>	455.0	<i>E1</i>	2.47±0.32	2.00	2.46	0.018
		0	0 0 <sup>+</sup>	508.2	<i>E1</i>	1	0	1	
571.7	0 3 <sup>-</sup>	174.1	0 4 <sup>+</sup>	397.6	<i>E1</i>	2.23±0.23	1.33	2.18	
		53.2	0 2 <sup>+</sup>	518.5	<i>E1</i>	1	1	1	
951.9	1 1 <sup>-</sup>	571.7	0 3 <sup>-</sup>	380.1	<i>E2</i>	0.22±0.07	0.67	0.22	-0.04
		508.2	0 1 <sup>-</sup>	443.8	<i>E2</i>	1	1	1	
971.7	1 2 <sup>-</sup>	571.7	0 3 <sup>-</sup>	399.8	<i>E2</i>	1.3 ±1.1	4.00	1.6	
		508.2	0 1 <sup>-</sup>	463.5	<i>E2</i>	1	1	1	
1079.2	2 2 <sup>-</sup>	781.4	2 2 <sup>+</sup>	297.8	<i>E1</i>	1	1	1	-0.04
		825.4	2 3 <sup>+</sup>	253.6	<i>E1</i>	≈ 0.34	0.50	0.3	
1127.9	2 3 <sup>-</sup>	781.4	2 2 <sup>+</sup>	346.9	<i>E1</i>	≤ 1.5	0.75	1.1	
		825.4	2 3 <sup>+</sup>	302.2	<i>E1</i>	1	1	1	

<sup>a</sup> The Mihailov formula [30] for the reduced transition probability, applied to the investigated cases, reads:  $B(L; K_i I_i \rightarrow K_f I_f) = \langle I_i L K_i K_f - K_i | I_f K_f \rangle^2 M^2 \{1 + [I_f(I_f + 1) - I_i(I_i + 1)] a\}^2$ , where  $M$ ,  $a$  are parameters of the theory. For  $a = 0$ , this formula is identical with that given by Alaga *et al.* [24].

The  $A_{12}$  value has been found from the analysis of the transitions to the levels of the  $K = 1$  and  $K = 2$  bands. These values of the matrix elements, Table V, are somewhat higher than those deduced from energy-spacing considerations.

The band-mixing effects discussed here are reflected also in the  $\gamma$ -ray branching ratios. The reduced branching ratios calculated for transitions de-exciting the negative-parity states deviate in most cases from the predictions of the Alaga [24] rule (transitions de-exciting the even-parity states have been already analysed in Table IV). Three groups of branching ratios, corresponding to transitions between three pairs of rotational bands, are analysed in Table VII. Deviations from the Alaga rule are clearly observed for two groups. For the third group, deviations are not obvious because of the large uncertainties in the experimental data. An adjustment of one parameter for each group provides agreement between the calculated and experimental branching ratios within experimental error.

The 366.5 keV (1<sup>-</sup>) level in  $^{230}\text{U}$  is believed to be a band-head state for the  $K^\pi = 0^-$  octupole band. The analogous 1<sup>-</sup> state in  $^{228}\text{Th}$ , the isotone of  $^{230}\text{U}$ , is observed at 328 keV.

8.3. Supplementary note

When preparation of the manuscript of the present work was almost finished, a publication by Lourens *et al.* [31] became available. These authors give the decay scheme of  $^{230}\text{Pa}$  based on studies of the singles  $\gamma$ -ray and electron spectra, and on the determination of the decay energies  $Q_{EC}$  and  $Q_{\beta^-}$ .

No coincidence measurements similar or equivalent to our  $e\text{-}\gamma$  studies were reported in their paper.

As mentioned earlier, our experiments were performed in part at the Joint Institute of Nuclear Research in Dubna and at the University of Aarhus. We are grateful to Professor G. N. Flerov and co-workers, and to Professor P. G. Hansen and his colleagues for their kind hospitality.

## REFERENCES

- [1] E. K. Hyde, I. Perlman, G. Seaborg, *The Nuclear Properties of the Heavy Elements*, Prentice-Hall INC 1964.
- [2] C. M. Lederer, J. M. Hollander, I. Perlman, *Table of Isotopes*, John Wiley, N. Y. 1967.
- [3] O. B. Nielsen, H. Nordby, S. Bjørnholm, unpublished results reported in: E. K. Hyde *et al.*, *ibid.*
- [4] W. Kurcewicz, K. Stryczniewicz, J. Żylicz, S. Chojnacki, T. Morek, I. Yutlandov, Contribution to the *Conf. on Nuclear Spectroscopy and Theory of Nucleus*, *JINR Report* 6-4756 p. 121, Dubna 1969.
- [5] J. P. Briand, P. Chevallier, J. Borg, M. J. Teillac, *CR Acad. Sci. (Paris)*, **B269**, 582 (1969).
- [6] W. Kurcewicz *et al.*, to be published.
- [7] M. W. Hill, *Thesis*, UCRL-8423 Report, NAS-NS 3016, 40 (1959).
- [8] S. Bjørnholm, E. R. Johansson, H. Nordby, *Nuclear Instrum. Methods*, **27**, 243 (1963).
- [9] S. M. Brahmavar, J. H. Hamilton, A. V. Ramayya, E. F. Zganjar, C. E. Bemis Jr., *Nuclear Phys.*, **A125**, 217 (1969).
- [10] A. Plochocki, E. Belcarz, M. Ślapa, M. Szymczak, J. Żylicz, *Nuclear Instrum. Methods*, to be published.
- [11] R. S. Hager, E. C. Seltzer, *Nuclear Data*, **4**, 1 (1968).
- [12] Z. Preibisz, W. Kurcewicz, A. Zgliniński, *Nukleonika*, **14**, 743 (1969).
- [13] A. H. Wapstra, G. J. Nijgh, R. van Lieshout, *Nuclear Spectroscopy Tables*, North-Holland Publ. Co., Amsterdam 1957.
- [14] L. N. Zyryanova, *Once Forbidden Beta Decay*, Pergamon Press, Oxford 1963.
- [15] A. Peghaire, *Nuclear Instrum. Methods*, **75**, 66 (1969).
- [16] J. O. Rasmussen, *Nuclear Phys.*, **19**, 85 (1960).
- [17] J. P. Davidson, *Collective Models of the Nucleus*, Academic Press, Inc., New York 1968.
- [18] W. R. Neal, H. W. Kraner, *Phys. Rev.*, **137**, B1164 (1965).
- [19] B. R. Mottelson, *Proc. Internal Conf. on Nuclear Structure*, Tokyo 1967.
- [20] S. F. Koksharova, V. M. Mihailov, Paper presented at the *19th Annual Conference on Nuclear Spectroscopy and Structure of Atomic Nucleus in Yerevan* (1969), unpublished.
- [21] E. Arbmán, S. Bjørnholm, O. B. Nielsen, *Nuclear Phys.*, **21**, 406 (1960).
- [22] S. Bjørnholm, F. Boehm, A. B. Kuntsen, O. B. Nielsen, *Nuclear Phys.*, **42**, 469 (1963).
- [23] S. Bjørnholm, J. Borggreen, D. Davis, N. J. S. Hansen, J. Pedersen, H. L. Nielsen, *Nuclear Phys.*, **A118**, 261 (1968).
- [24] G. Alaga, K. Alder, A. Bohr, B. Mottelson, *Mat. Fys. Medd. Dan. Vid. Selsk.*, **29**, No. 9 (1955).
- [25] P. G. Hansen, O. B. Nielsen, R. K. Sheline, *Nuclear Phys.*, **12**, 389 (1959).
- [26] K. M. Zheleznova *et al.*, *JINR Report* D-2157, Dubna 1965.
- [27] J. Błocki, W. Kurcewicz, *Phys. Letters*, **30B**, 458 (1969).
- [28] K. Neergård, P. Vogel, *Nuclear Phys.*, **A149**, 217 (1970).
- [29] A. L. Komov, L. A. Malov, V. G. Soloviev, *Report* P4-5126,, Dubna 1970.
- [30] V. M. Mihailov, *Izv. Akad. Nauk SSSR, Ser. Fiz.*, **30**, 1334 (1966).
- [31] W. Lourens, B. O. Ten Brink, A. H. Wapstra, *Nuclear Phys.*, **A152**, 463 (1970).